The EMBO Journal vol.3 no.8 pp.1831 – 1836, 1984

Nucleo-cytoplasmic flux and intracellular mobility in single hepatocytes measured by fluorescence microphotolysis

R. Peters

Max-Planck-Institut für Biophysik, Kennedy-Allee 70, 6000 Frankfurt 70, FRG

Communicated by D. Oesterhelt

Fluorescence microphotolysis was used to measure nucleo-cytoplasmic flux in single rat hepatocytes for a series of dextrans ranging in molecular mass from 3 to 150 kd. The cytoplasmic translational diffusion coefficient D_C and the nucleoplasmic diffusion coefficient D_N of a 62-kd dextran were also determined. D_C was $\sim 2 \times 10^{-8}$ and D_N $\sim 3 \times 10^{-8}$ cm²/s, i.e., 1/20 – 1/15 of the value in free solution. The mobile fraction amounted to 0.7 – 0.8 in measurements of both intracellular diffusion and nucleo-cytoplasmic flux. The flux of dextrans from cytoplasm to nucleus depended inversely on molecular mass with an exclusion limit between 17 and 41 kd suggesting that the nuclear envelope has functions of a molecular sieve. Employing the Pappenheimer-Renkin equations, a functional pore radius of 50 – 56 Å was derived. By comparison with recent measurements on isolated liver cell nuclei, large quantitative differences between the intracellularly located and the isolated nucleus were revealed.

Key words: dextran/hepatocyte/intracellular transport/nuclear envelope/photobleaching

Introduction

In the eukaryotic cell the nuclear envelope mediates the exchange of instructive and regulative molecules between genetic material and cytoplasm. However, knowledge of nucleo-cytoplasmic transport is 'anecdotal rather than systematic' (Paine and Horowitz, 1980). In the past, technical difficulties arose in particular from the small dimensions of average cells and from the intimate integration of the nucleus into the cellular architecture. Most data were obtained from studies of extremely large cells such as amphibian oocytes. With these cells microinjection could be combined with electron microscopy (Feldherr, 1965), fluorescence microscopy (Paine, 1975) and various techniques based on radiotracers (Bonner, 1975; Paine *et al.*, 1975; De Robertis *et al.*, 1978). Paine *et al.* (1975) injected radiolabeled dextrans into frog oocytes and followed their spreading in the cytoplasm and across the nuclear envelope by cryofixation and microautoradiography. Thus, the cytoplasmic diffusion coefficient and the permeability coefficient of the nuclear envelope could be determined for a series of homologous molecules with graded molecular size. Dextrans are of advantage in such studies because they are spherical, hydrophilic molecules which are not or little degraded or bound in the cell.

Recently, fluorescence microphotolysis (for review, see Peters, 1983a) has been employed in a manner permitting measurement of the transfer of fluorescent solutes through membranes in single cells and organelles (Peters, 1983b, 1984). The permeability of the nuclear envelope to fluorescently labeled dextrans was measured in isolated liver cell nuclei (Peters, 1983b) and nuclear ghosts (Lang and Peters, 1984). By injecting dextrans into cultured rat liver cells we have now studied the permeability properties of the nuclear envelope in the living cell. For the first time rate constants of nucleo-cytoplasmic flux as well as cytoplasmic and nucleoplasmic diffusion coefficients have been measured in a normal-sized cell (see Kohen *et al.*, 1971 for a remarkable precursor). The results confirm earlier notions (Feldherr, 1965; Paine *et al.*, 1975) that the nuclear envelope has the functions of a molecular sieve which can be adequately characterized by a functional pore radius (Pappenheimer *et al.*, 1951; Renkin, 1954). However, large quantitative differences between cultured liver cells and isolated nuclei (Peters, 1983b) were observed.

Results

The light-microscopic appearance of hepatocytes cultured for 12 – 36 h after isolation is shown in Figure 1. Immediately after isolation the cells were spherical and highly refractile. After some hours of cultivation, however, the cells spread on the bottom of the plastic dish and assumed an extended and flattened geometry. Occurring in strings and small colonies, the cells featured a polygonal circumference with diameters of 50 – 100 μm. The nucleus – initially spherical with an average diameter of 8 μm – also flattened and the larger (horizontal) diameter was 12 – 20 μm. Assuming that the nuclear volume remained approximately constant the smaller (vertical) diameter of the nuclei is estimated to be only 1 – 2 μm. In the hepatocyte within the liver parenchyma the nuclear volume amounts to 5 – 10% of the cellular volume (Novikoff and Holtzman, 1970). This ratio – favorable for measurements of nucleo-cytoplasmic flux – was obviously maintained in cultured cells. In the cultured cell the nucleus is

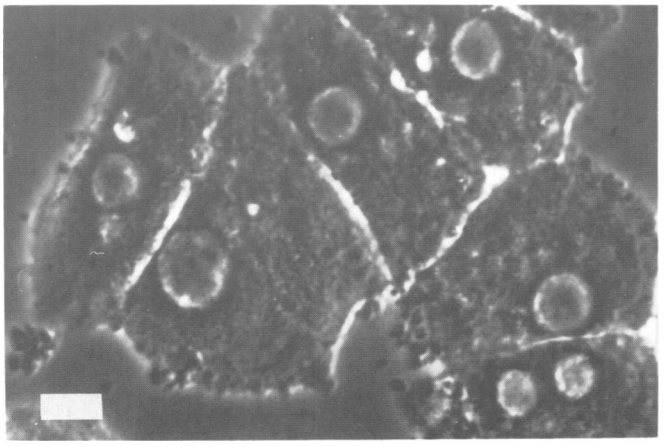

Fig. 1. Microphotograph of hepatocytes in primary culture ~12 – 36 h after isolation. Bar = 10 μm.

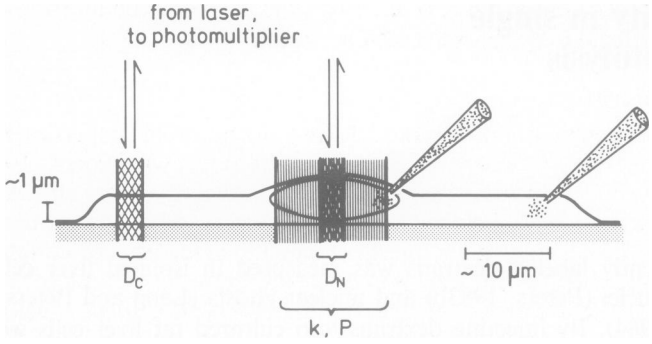

Fig. 2. Schematic cross-section of hepatocyte. The sites of microinjection and the location and geometry of the laser beam employed in measurements of D_C, the cytoplasmic translational diffusion coefficient, D_N, the nucleoplasmic diffusion coefficient, k, the rate constant of nucleo-cytoplasmic flux, and P, the permeability coefficient, are indicated.

clearly visible and rather lucid whereas the cytoplasm, packed with inclusions (mitochondria, ribosomes, glycogen granula, etc.), is more refractile.

Based on light microscopy and fluorescence scans (Figure 3, discussed below) an approximate cross-section of the liver cell in culture was constructed (Figure 2). The sites of microinjection are indicated. Injection into the cytoplasm was usually tolerated by the cells without morphological changes if the injected volume was in the order of 100 fl, i.e., only a few percent of the cellular volume. Injection into the nucleus was technically easy but did not always result in a tight nucleus. However, in a substantial fraction of experiments involving the (non-permeating) 62-kd dextran (FD70) nuclear fluorescence remained stable over an extended time period. Such nuclei were considered tight and subjected to measurements of intra-nuclear diffusion. In Figure 2 the sites and geometries of the laser beam employed in measurements of the cytoplasmic translational diffusion coefficient D_C, the intra-nuclear diffusion coefficient D_N, and the rate constant k and the permeability coefficient P of nucleo-cytoplasmic flux, respectively, are also shown.

Abbreviations and some properties of the fluorescein isothiocyanate-labeled dextrans used in this study are given in Table II. After injection into the cytoplasm two categories of dextrans were distinguished by fluorescence microscopy: FD3, FD10, and FD20 permeated into, whereas FD40, FD70, and FD150 were excluded from the nucleus. This observation was quantified by scanning cells for fluorescence. Figure 3 shows scans after injection of the smallest (FD3, panel a) and largest (FD150, panel b) dextran. The scans in Figure 3 were obtained ~5 min after injection. Repetitive scanning (not shown) revealed the fluorescence pattern to remain constant over a period of at least 30 min although a slight uniform decrease of fluorescence (<10% in 30 min) was sometimes observed. Assuming that the many parameters which, in general, modify fluorescence (e.g., scattering, adsorption to or exclusion from cytoplasmic structures, local pH differences) can be, to a first approximation, neglected, the scans may be used to estimate roughly the relative thickness of the cytoplasmic layer embedding the nucleus. According to this criterion, the cytoplasm – in the nuclear region – occupies only 10–30% of the cellular vertical diameter.

The interpretation of flux measurements by fluorescence microphotolysis is simple if diffusion is fast as compared with membrane permeation (see Materials and methods).

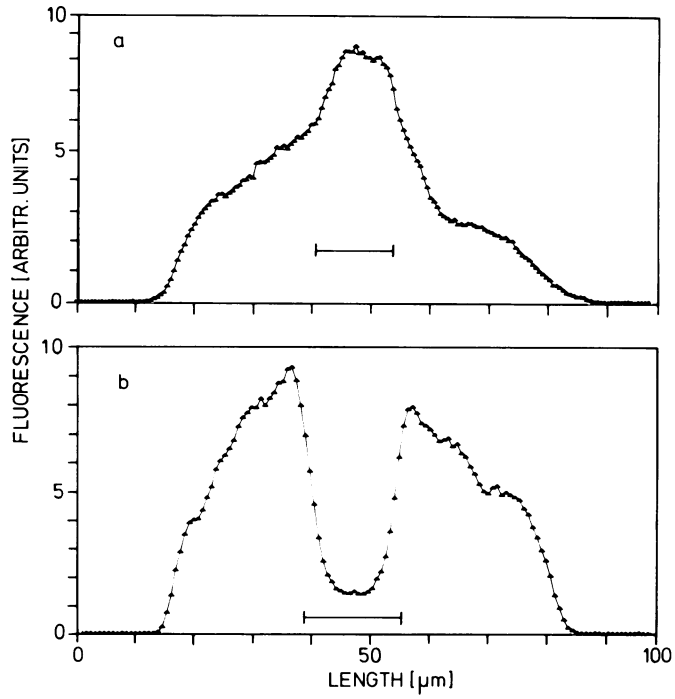

Fig. 3. Fluorescence scans of hepatocytes after injection of **(panel a)** a small, 3-kd and **(panel b)** a large, 150-kd dextran into the cytoplasm. The scans are through the center of the nuclei whose position is indicated by the bar.

Therefore, the diffusion coefficient of FD70 was measured in both cytoplasm and nucleus (Figure 4 and Table I). As compared with free solution, the cytoplasmic diffusion coefficient is smaller by a factor of 20. Previous measurements of diffusion in the cytoplasm by the same or other methods have yielded comparable results. The self-diffusion coefficient of water was reduced in human red cells to 20% and in yeast to 15% of the value of pure water (Tanner, 1983). Similarly, the diffusion coefficient of a number of mono-, oligo- and polysaccharides in the cytoplasm of amphibian oocytes and other large cells amounted to 20–50% of the value in free solution (for review, see Paine and Horowitz, 1980). The diffusion coefficient of bovine serum albumin (BSA) was restricted more extensively in the cytoplasm of human fibroblasts amounting to 1×10^{-8} cm²/s as compared with 68×10^{-8} cm²/s in free solution (Wojcieszyn *et al.*, 1981). Diffusion in the nucleoplasm, to our knowledge, has not been measured before. Our results show diffusion to be substantially faster in the nucleo- than in the cytoplasm. Thus, although loaded with macromolecules, the nucleus has an elaborate architecture allowing for rapid translational diffusion. Such an organization is consistent with electron microscopy revealing a system of intranuclear channels (Schatten and Thoman, 1978) and certainly facilitates gene activity. Diffusion in the cyto- and nucleoplasm will be discussed in detail elsewhere (Peters, unpublished results). For the present purpose it is sufficient to note that diffusion is indeed fast as compared with nucleocytoplasmic flux (see Materials and methods for a quantitative criterion). Nevertheless, in flux measurements of FD20, the largest of the permeable dextrans, an initial fast phase was apparent (Figure 5) which we attribute to diffusional redistribution in the cytoplasm after photobleaching.

Measurements of nucleo-cytoplasmic flux are summarized in Table II. Raw data (Figure 5, upper panel) were analyzed

for a mobile and an immobile fraction as described under Materials and methods. After replotting data according to Equation 2 (Figure 5, lower panel) a linear regression analysis was performed and the rate constant k determined. Usually, an excellent fit was obtained in this manner. The curves of FD20 (curve c in Figure 5, lower panel) were characterized by a fast initial phase which, as mentioned above, may be attributed to the initial redistribution in the cytoplasm. The mobile fraction amounted to 0.7 – 0.8, i.e., to a similar value as in measurements of intracellular diffusion. Diffusion coefficients of dextrans were also measured in free solution and, employing Stoke's relationship, hydrodynamic radii were derived (Table II). With one exception (FD3) these diffusion coefficients and molecular radii are in excellent agreement with published values (Granath and Kvist, 1967). FD3 easily forms dimers (Paine *et al.*, 1975) which could account for the diffusion coefficient measured in this study.

Discussion

Molecular sieving is one of the best documented properties of the nuclear envelope although previous experiments, for technical reasons, were confined to extremely large cells. As early as 1965, Feldherr showed by electron microscopy that colloidal gold, after injection into the cytoplasm of certain unicellular organisms, was excluded from the nucleus if the particle diameter exceeded 125 – 157 Å (Feldherr, 1965). Similarly, ferritin (diameter 95 Å) was restricted to the cytoplasm of oocytes whereas smaller proteins could penetrate into the nucleus (Paine and Feldherr, 1972). In

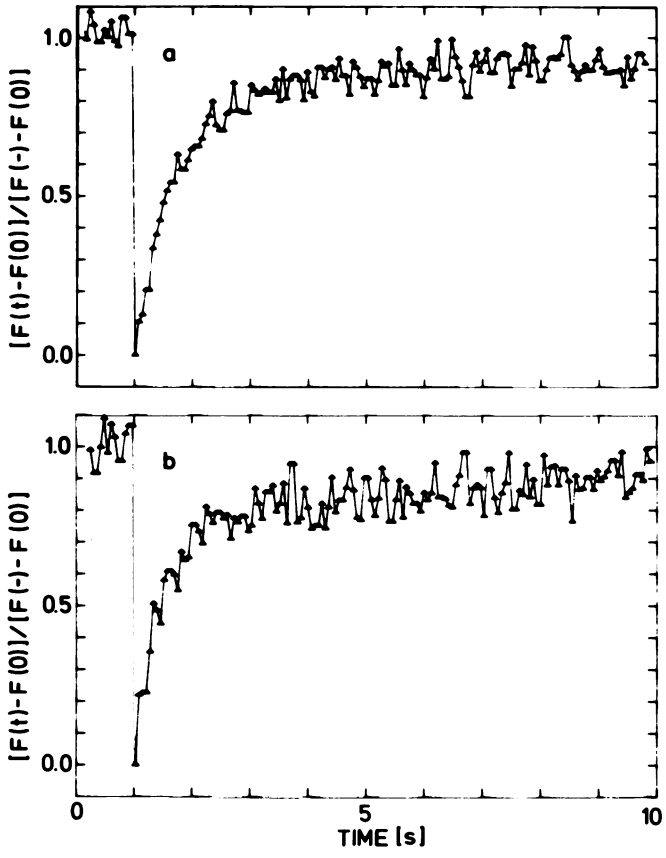

Fig. 4. Translational mobility of a 62-kd dextran in the cytoplasm (**panel a**) and in the nucleoplasm (**panel b**). The three steps of the measurement are clearly seen: measurement of fluorescence before bleaching, reduction of fluorescence by bleaching and redistribution of fluorescence after bleaching. The illuminated area had a radius of 2.0 μm. Diffusion coefficients are ~2 x 10^{-8} (**panel a**) and 3 x 10^{-8} (**panel b**) cm²/s.

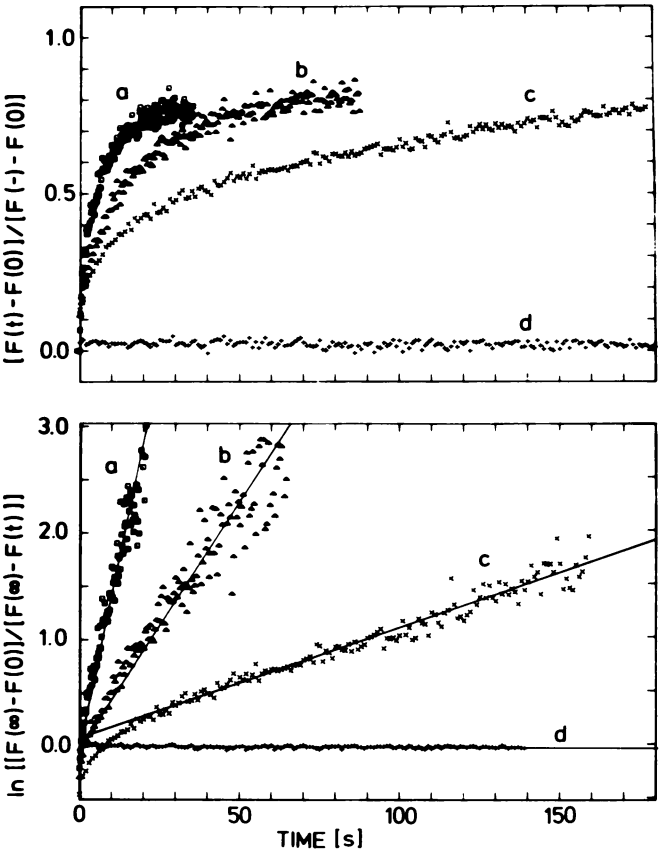

Fig. 5. Nucleo-cytoplasmic flux of dextrans having a molecular mass of (**a**) 2.9, (**b**) 10.5, (**c**) 17.5, and (**d**) 41.0 kd. In the upper panel the raw data are given in a normalized form. The three steps of the measurement are: measurement of intranuclear fluorescence before bleaching (normalized fluorescence = 1.0), reduction of fluorescene by bleaching (normalized fluorescence = 0.0), and recovery of fluorescence by influx of dextrans from cytoplasm to nucleus. In the lower panel the data have been replotted according to Equation 2 and fitted by linear regression.

Table I. Diffusive mobility of a 62-kd dextran in free solution and in cultured liver cells[a]

In free solution[b]		In the cytoplasm		In the nucleoplasm	
D_W 10^{-8} cm²/s	$R_{M,W}$	D_C 10^{-8} cm²/s	$R_{M,C}$	D_N 10^{-8} cm²/s	$R_{M,N}$
39.0 ± 2.6	1	1.97 ± 0.34	0.87 ± 0.14	2.86 ± 0.95	0.84 ± 0.07

[a]Mean ± S.D. of 5 – 10 measurements.
[b]1 μM solution in 7 mM sodium phosphate buffer, pH 7.4.

Table II. Nucleo-cytoplasmic flux of dextrans in cultured rat liver cells

Abbreviation of dextran	Mean mol.mass kd	Diffuson coefficient[a] 10^{-8} cm²/s	Stokes radius[b] Å	Rate constant[c] s^{-1}	Mobile fraction	n^c
FD3	2.9[d]	97.8 ± 6.0[d]	22.0[d]	0.1885 ± 0.0822	0.69 ± 0.09	22
FD10	10.5	75.7 ± 2.5	28.3	0.0487 ± 0.0191	0.69 ± 0.14	24
FD20	17.5	65.1 ± 6.5	33.0	0.0196 ± 0.0067	0.76 ± 0.24	16
FD40	41.0	46.3 ± 4.6	46.4	−0.0014 ± 0.0052		18
FD70	62.0	39.0 ± 2.6	55.1	0.0007 ± 0.0021		11
FD150	156.9	23.7 ± 1.3	90.7			

[a]1 μM solution in 7 mM sodium phosphate buffer, pH 7.4.
[b]Calculated according to radius a = $(kT)/(6\pi\eta D)$, where k = Boltzmann's constant, T = absolute temperature, and η = solvent viscosity.
[c]Mean ± S.D. of n measurements; in the case of FD40 and FD70 the calculation was based on an assumed mobile fraction of 1.0.
[d]FD3 may occur as a dimer in solution as discussed in the text.

Table III. Permeability properties of the nuclear envelope in cultured liver cells and isolated nuclei

		Cultured rat liver cell	Isolated nucleus[a]
Rate constant of the ~20-kd dextran	(s^{-1})	0.0196 ± 0.0067	0.53 ± 0.22
Permeability coefficient of the 20-kd dextran[b]	(10^{-8} cm/s)	261	7050
Exclusion limit for dextrans	(kd)	17–41	62–156
Functional pore radius[c]	(Å)	50–56	56–59

[a]Data are from Peters (1983b).
[b]Calculated according to Equation 3 using the same volume/area ratio (4/3 μm) for both intact cell and isolated nucleus.
[c]Calculated according to Equations 7 and 8.

salivary gland cells of *Chironomus* larvae the accessibility of the nucleoplasm to a number of fluorescein-isothiocyanate-labeled compounds was studied by flourescence microscopy and found to depend strongly on molecular size: BSA (diameter ~70 Å) was virtually excluded from the nucleus whereas ovalbumin (54 Å) and smaller molecules penetrated into the nucleus (Paine, 1975). Comparable results were obtained by radio-tracer methods for *Xenopus* oocytes (Bonner, 1975). Paine *et al.* (1975) measured the distribution of radioactively-labeled dextrans in frog oocytes by autoradiography and derived a value for the functional pore radius (to be discussed below). The present study shows that the nuclear envelope of the hepatocyte – the cell used most frequently in biochemical studies of the nuclear envelope – also has properties of a molecular sieve. In this normal-sized cell nucleo-cytoplasmic flux depends also inversely on molecular size. The exclusion limit for dextrans is 17–41 kd.

If membrane transport occurs via a homogeneous population of water-filled cylindrical pores the flux of spherical hydrophilic solutes can be used to derive the pore radius (Pappenheimer *et al.*, 1951; Renkin, 1954; for review, see Paine and Scherr, 1975). We have used Renkin's equation in a form (Peters, 1983b) not requiring the explicit knowledge of nuclear volume, surface area and pore length. Applied to the present measurements (Table II) the functional pore radius is calculated from Equations 7 and 8 to be 49.5 Å (combining FD3 and FD10 data), 51.5 Å (FD3 and FD20 data), or 55.5 Å (FD10 and FD20 data). As mentioned under Materials and methods the Renkin-equation is an approximation whereas a more rigorous solution has been provided by Haberman and Sayre (1958) and tabulated by Paine and Scherr (1975). With that approach the functional pore radius becomes somewhat larger, namely 53 Å (FD3 and FD10), 57 Å (FD3 and FD20) or 61 Å (FD10 and FD20). If the pore radius is known the flux of a solute can be predicted. Thus, using a mean functional pore radius of 52 Å and applying Equations 7 and 8, the rate constant of FD40 is predicted to be 0.0008 s^{-1}, i.e., well within the experimentally determined value of −0.0014 ± 0.0052 s^{-1}. The area density of pores may be calculated only if the pore length, in addition to the pore radius, is known. The pore length, however, is a source of considerable uncertainty. In the calculation of the functional pore radius Paine *et al.* (1975), for instance, used a value of 1500 Å. That figure is based on electron microscopic measurements and, including pore complex, nuclear lamina and outer parts of the intranuclear channels (Schatten and Thoman, 1978), may be regarded as an upper limit. Recent structural data showing the pore complex of *Xenopus* oocytes at a resolution of 90 Å (Unwin and Milligan, 1982) suggest a pore length of ~300 Å. Using that value the area density of functional pores is calculated from Equation 9 to be ~10 μm^{-2}. For comparison the density of the pore complex in hepatocytes, as determined by electron microcopy, may be quoted; it is 14–16 μm^{-2} (Franke *et al.*, 1971; Maul, 1977).

Paine *et al.* (1975), using the equations of Haberman and Sayre (1958) and a pore length of 1500 Å, determined the functional pore radius of the nuclear envelope in frog oocytes to be ~45 Å. To facilitate a direct comparison with the present study we have recalculated the pore radius using the data of Paine *et al.* (1975) and our Equations 7 and 8. Determined in this manner the pore radius centers around 36 Å (31.5 Å combining data of the 12.0 Å and the 23.3 Å dextran, 37.5 Å for the 12.0 Å and 35.5 Å dextran, and 38.5 Å for the 23.3 Å and 35.5 Å dextran). Thus, a relatively large difference between functional pores in the nuclear envelope of frog oocytes and cultured liver cells seems to exist and may indicate, in spite of the widely differing experimental methods, a true difference.

Comparing now the present results with those obtained recently for isolated nuclei (Peters, 1983b) it may be recalled that the investigations relate to similar but not identical material. In Peters (1983b) nuclei were isolated from rat liver tissue, whereas the present study pertains to rat liver cells kept for 12–36 h in culture. Much evidence suggests that the liver cell retains several of its specific functions in culture, e.g., the ability to form biliary canaliculi (Gebhardt and Jung, 1982) and to produce and secrete serum proteins including albumin (Sirica *et al.*, 1979). On the other hand, in culture the liver cell acquires a number of features characteristic of fetal hepatocytes (for review, see Pitot and Sirica, 1980). Qualitatively, the permeability properties of the nuclear envelope in the cell and *in vitro* are similar (Table III). There is a strong dependence of solute flux on molecular size which, in both cases, can be satisfactorally accounted for by assuming the existence of pores. In the cell, the functional pore radius is ~5 Å smaller than in the isolated nucleus. Correspondingly, the exclusion limit is shifted to markedly smaller mol. wts. than in the isolated nucleus. A large difference exists in the absolute flux rates. The permeability coefficient of FD20, for instance, is ~30-fold larger in the isolated nucleus. In the framework of the pore hypothesis this could be accounted for by a much larger area density of functional pores in the isolated nucleus.

Molecular sieving may be the best characterized function of the nuclear envelope. It is by no means, however, its single or most important feature. We believe that the topographic position of the nuclear envelope between nucleus and cytoplasm, i.e., between genetic material and protein synthesizing apparatus, is an intimation of regulatory functions in gene expression. Data in this field are scarce and knowledge is indeed anecdotal. One intention of this communication was to show how the problem may be approached in the future.

Materials and methods

Dextrans

Abbreviations, molecular weights and other properties of the fluorescein isothiocyanate-labeled dextrans used in this study are given in Table II. FD3 was obtained from Pharmacia (Freiburg, FRG), FD10, FD20, FD40, FD70, and FD150 were from Sigma (Taufkirchen, FRG). The degree of labeling was 0.004–0.01 mol of fluorescein isothiocyanate/mol of glucose residue.

Isolation and cultivation of rat liver cells

Hepatocytes were isolated by the collagenase perfusion method (Howard *et al.*, 1967; Berry and Friend, 1969; reviewed by Seglen, 1976) incorporating most of the modifications described by Gebhardt and Mecke (1979) and Gebhardt and Jung (1982). Sprague-Dawley rats (200–300 g) were kept on a standard diet and tap water. After anaesthesia with sodium pentobarbital (40 mg/kg body weight) a laparascopy was performed under sterile conditions. Heparin (1250 IU) was injected into the Vena iliolumbalis dextra. A cannula was inserted into the Vena portae and the liver perfused for some minutes with a calcium-free perfusion buffer containing 5.36 mM KCl, 0.77 mM $MgSO_4$, 0.93 mM $MgCl_2$, 0.34 mM Na_2HPO_4, 0.44 mM KH_2PO_4, 0.2 mM EGTA, 10 mM Hepes, and 145 mM NaCl, pH 7.4. The liver was removed. In a recirculation system the liver was perfused for another 5–15 min at a rate of ~50 ml/min with 80 ml of the same buffer supplemented, however, with glucose (2 g/l), BSA (2 g/l), $CaCl_2$ (2 mM), and collagenase (50 mg/80 ml, type I of Sigma, Taufkirchen, FRG). The recirculation system consisted of a peristaltic pump, an oxygenator where the perfusate was equilibrated with oxygen and warmed to 37°C, and a bubble trap. After perfusion, the liver was transferred into 100 ml of an isolation buffer containing NaCl (137 mM), KCl (5.4 mM), $MgSO_4$ (1.17 mM), KH_2PO_4 (0.15 mM), Na_2HPO_4 (0.79 mM), Hepes (10 mM), $CaCl_2$ (1 mM), and glucose (1 g/l), pH 7.4. The liver capsule was opened and the cells liberated by gently shaking the liver in the buffer. Connective tissue was discarded and the cells repeatedly washed in isolation buffer by centrifugation at ~100 *g*. The cells were counted and subjected to a trypan blue exclusion test. The viability was usually around 80%. The cells were taken up in Williams medium E (Flow Laboratories, Bonn, FRG) with 10% foetal calf serum (Sebio, Walchsing, FRG), plated in 30 mm plastic Petri dishes, and cultured at 37°C in an atmosphere containing 5% CO_2. The medium was changed 2–4 h after plating. Flux and diffusion measurements were all performed on cells cultured for ~12–36 h.

Microinjection

Dextrans were introduced into hepatocytes by pressure injection. Capillaries (Clark Electromedical Instruments, Pangbourne, UK, No. GC 100 TF-10) were cleaned and drawn without pre-pulling to a tip diameter of ~0.5–1.0 μm. The capillaries were filled with 3 μl of a solution of dextran in jection buffer containing 48 mM K_2HPO_4, 14 mM NaH_2PO_4, and 4.5 mM KH_2PO_4, pH 7.2. The concentration of dextrans was 10 g/l, i.e., ~0.07–3.3 mM depending on molecular mass. Before use the dextran solution were centrifuged for 30 min at ~100 000 *g*. A filled capillary was inserted into the needle holder of a micromanipulator (Leitz, Wetzlar, FRG) and connected to a pressure system as described by Ansorge (1982). The hepatocytes were washed with isolated buffer in the culture dish and placed on the stage of the fluorescence microscope. Microinjection was performed by inserting the tip of the capillary into the cell and applying the injection pressure for some seconds. The injection pressure had been adjusted such that the injected volume amounted to ~100 fl, i.e., a few percent of the cellular volume. The capillary was withdrawn and the cell allowed to equilibrate for some minutes before starting the measurements.

Instrumentation for fluorescence microphotolysis

The equipment has been described before (Peters and Richter, 1981; Peters, 1984). It consisted mainly of an argon laser, a fluorescence microscope with vertical illuminator, scanning stage and photometric attachment, a single-photon counting system, and a computer.

Diffusion measurements

The measurement of translational diffusion coefficients by fluorescence microphotolysis was performed as described previously (for review, see Peters, 1983a). The 476.5 nm laser line was used at 200 mW. In measurements involving liver cells a diaphragm was placed at an image plane in front of the vertical illuminator by which means the central part of the beam was cut out and – focussed into the specimen by a 40-fold, n.a. 0.60 phase contrast objective lens – yielded a homogeneously illuminated area of 2.0 μm radius. Diffusion coefficients of dextrans in free solution were measured by pre-focussing the beam with a 600 mm plano-convex lense and imaging the laser waist into the specimen with a 16-fold objective lens. This yielded an illuminated area of Gaussian intensity profile and an e^{-2} radius of 18.5 μm. The dextrans were dissolved at a concentration of 1 μM in 7 mM sodium phosphate buffer, pH 7.4, and placed as a very thin layer between a glass slide and a cover slip which was carefully sealed at the edges with silicon grease. Diffusion data were analysed by determination of the half-time of fluorescence recovery. The diffusion coefficient was calculated from the half-time using equation 19 of Axelrod *et al.* (1976) with the appropriate gamma-value.

Flux measurements

The methodological basis of flux measurement by fluorescence microphotolysis has been described recently (Peters, 1983b, 1984). When applied to single organelles the principle of the method is to equilibrate organelles with a fluorescent solution, to deplete a single organelle from fluorescence by a high-intensity pulse of a laser beam focussed into the interior of the organelle and to measure the influx of solute by microfluorometry. The procedure yields simple kinetics if diffusion in the medium both outside and inside the organelle is fast as compared with transport through the membrane. As discussed in Peters (1984) this is frequently the case. For a sphere the condition is fulfilled (Fenichel and Horowitz, 1969) if $D \geq 10\,R\,P$ where D is the diffusion coefficient of the solute, R is the radius of the sphere, and P is the membrane permeability coefficient. Influx kinetics are analyzed for two components, a mobile and an immobile fraction. If the external volume is much larger than the internal volume the magnitude R_M of the mobile fraction is given by:

$$R_M = (F(\infty) - F(0))/(F(-) - F(0)) \quad (1)$$

where $F(-)$, $F(0)$ and $F(\infty)$, respectively, is the fluorescence signal before, immediately after and a long time after the photolysing laser flash, respectively. An immobile fraction ($1 - R_M$) may arise from adsorption of solute to the surface membrane (Peters, 1984) or to intracellular immobile components (Peters, 1983b). In case of a simple passive mechanism of membrane transport in which the flux is proportional to the concentration difference over the membrane, the kinetics of fluorescence recovery are given by:

$$\ln((F(\infty) - F(0))/(F(\infty) - F(t))) = kt \quad (2)$$

where $F(t)$ is the fluorescence signal at time t and k is the rate constant of in-

flux. The rate constant is related to the membrane permeability coefficient P by:

$$P = (V/S)k \quad (3)$$

where V and S are volume and surface area of the organelle, repectively. In case of a sphere $V/S = R/3$. Frequently, the $F(\infty)$ value can be read directly from the measuring curve. In some cases – if influx does not reach equilibrium during the measuring time – $F(\infty)$ may be determined by an appropriate computer curve fitting procedure (Peters, 1984). For determination of k, the raw data are usually plotted in a semi-logarithmic form according to Equation 2 and fitted by a linear regression analysis.

In the present flux measurements, a homogeneously illuminated area of 5.0 μm diameter was employed. The objective lens was a 40-fold, n.a. 0.60 plano-achromate. The illuminating beam had a full-angle divergence of ~30°. Over the cross-section of the cells (1–3 μm) the beam was therefore essentially a cylinder as indicated in Figure 2. In the photometric attachment a diaphragm of approximately the same radius as the image of the illuminated area was used to reject much of the fluorescence from areas other than the focal plane. All measurements were performed at ambient temperature (~22°C).

In the cases of FD40 and FD70 which do not (or very slowly) permeate into the nucleus a different procedure, not involving photobleaching, was adopted. Immediately after microinjection fluorescence was measured in an area close to the nucleus and taken as $F(-)$. Then, fluorescence was continuously recorded in the nuclear region and taken as $F(t)$. Since fluorescence in the nucleus increased only slowly with time and equilibrium was never reached, evaluation of the data in terms of a rate constant k (deliberately) assumed a mobile fraction $R_M = 1.0$. The procedure, of course, provides only an estimate of k because there is a time lag of ~15 s between injection and $F(-)$ measurement and because recording of $F(t)$ starts only ~30 s after injection.

Calculation of the functional pore radius

If a species of spherical molecules of radius a traverses a membrane by diffusion through a homogeneous population of water-filled cylindrical pores of area A_0, radius r, and length Δx the flux $\Delta m/\Delta t$ is given according to Fick's first law by:

$$\Delta m/\Delta t = D\, n\, A_{eff}\, \Delta C/\Delta x \quad (4)$$

where n is the area density of pores, A_{eff} is the pore area accessible to the molecular species and ΔC is the concentration difference. Hence,

$$P = D\, n\, A_{eff}/\Delta x \quad (5)$$

The restriction of diffusion through cylindrical pores (Pappenheimer *et al.*, 1951; Renkin, 1954; for review, see Paine and Scherr, 1975) has been attributed to two parameters: steric hindrance at the pore entry and viscous drag in the pore. Both parameters can be subsumed in the effective pore area A_{eff} which, in the case of no solvent flow, is related to the geometric pore area A_0 by:

$$A_{eff}/A_0 = (1 - a/r)^2\, g(a,r) \quad (6)$$

According to Renkin (1954) the wall drag factor $g(a,r)$ is closely approximated by:

$$g(a,r) = (1 - 2.104(a/r) + 2.09(a/r)^3 - 0.95(a/r)^5) \quad (7)$$

A more rigorous theoretical solution of the problem was provided by Haberman and Sayre (1958) and tabulated by Paine and Scherr (1975).

As described previously (Peters, 1983b), Equation 6 permits calculation of the effective pore radius from data of any two solutes i and j:

$$(k_i/D_i)/(k_j/D_j) = ((1 - a_i/r)^2 g(a_i,r))/((1 - a_j/r)^2 g(a_j,r)) \quad (8)$$

The area density n of pores can only be calculated if both pore area and length are known (or if one parameter is known and the other one can be reasonably estimated). Then, by combination of Equations 5 and 6,

$$n = (P\Delta x)/(D\, \pi\, r^2 (1 - a/r)^2\, g(a,r)) \quad (9)$$

Fluorescence scans

Scans were obtained by moving cells on a linear pathway through an illuminated area of 1.25 μm radius at constant speed (2.5 μm/s).

Photographs

Microphotographs were obtained on Agfapan 25 film employing 2 s exposure time.

Acknowledgements

I should like to thank Dr. R. Gebhardt and Professor D. Mecke for an introduction to the isolation and cultivation of hepatocytes and for sharing their vast experience in this field with us. Many thanks are due to Mrs. Daniela Gahl for collaboration and excellent support. Financial support by the Deutsche Forschungsgemeinschaft is gratefully acknowledged.

References

Ansorge,W. (1982) *Exp. Cell Res.*, **140**, 31-37.
Axelrod,D., Koppel,D.E., Schlessinger,J., Elson,E. and Webb,W.W. (1976) *Biophys. J.*, **16**, 1055-1069.
Berry,M.N. and Friend,D.S. (1969) *J. Cell Biol.*, **43**, 506-520.
Bonner,W.M. (1975) *J. Cell Biol.*, **64**, 421-430.
De Robertis,E.M., Langthorne,R.F. and Gurdon,J.B. (1978) *Nature*, **272**, 254-256.
Feldherr,C.M. (1965) *J. Cell Biol.*, **25**, 43-51.
Fenichel,I.R. and Horowitz,S.B. (1969) in Dowben,R.M. (ed.), *Biological Membranes*, Little, Brown and Comp., Boston, pp. 177-221.
Franke,W.W., Kartenbeck,J. and Deumling,B. (1971) *Experientia*, **27**, 372-373.
Gebhardt,R. and Mecke,D. (1979) *Exp. Cell Res.*, **124**, 349-359.
Gebhardt,R. and Jung,W. (1982) *Eur. J. Cell Biol.*, **69**, 68-76.
Haberman,W.L. and Sayre,R.M. (1958) *Motion of Rigid and Fluid Spheres in Stationary and Moving Liquids Inside Cylindrical Tubes*, David Taylor Model Basin. Report No. 1143. U.S. Navy, Washington, DC.
Granath,K.A. and Kvist,B.E. (1967) *J. Chromatogr.*, **28**, 69-81.
Howard,R.B., Christensen,A.K., Gibbs,F.A. and Pesch,L.A. (1967) *J. Cell Biol.*, **35**, 675-684.
Kohen,E., Siebert,G. and Kohen,C. (1971) *Hoppe-Seyler's Z. Physiol. Chem.*, **352**, 927-937.
Lang,I. and Peters,R. (1984) in Helmreich,H.J. (ed.), *Information and Energy Transfer in Biological Membranes*, Alan R. Liss, NY, in press.
Maul,G.G. (1977) *Int. Rev. Cytol.*, suppl. **6**, 76-186.
Novikoff,A.B. and Holtzman,E. (1976) *Cells and Orangelles*, 2nd edition, published by Holt, Rinehardt and Winston, NY.
Paine,P.L. (1975) *J. Cell Biol.*, **66**, 652-657.
Paine,P.L. and Feldherr,C.M. (1972) *Exp. Cell Res.*, **74**, 81-98.
Paine,P.L. and Scherr,P. (1975) *Biophys. J.*, **15**, 1087-1091.
Paine,P.L. and Horowitz,S.B. (1980) in Prescott,D.M. and Goldstein,L. (eds.), *Cell Biology*, Vol. **4**, Academic Press, NY, pp. 299-338.
Paine,P.L., Moore,L.C. and Horowitz,S.B. (1975) *Nature*, **254**, 109-114.
Pappenheimer,J.R., Renkin,E.M. and Borrero,L. (1951) *Am. J. Physiol.*, **167**, 12-31.
Peters,R. (1983a) *Naturwissenschaften*, **70**, 294-302.
Peters,R. (1983b) *J. Biol. Chem.*, **258**, 11427-11429.
Peters,R. (1984) *Eur. Biophys. J.*, in press.
Peters,R. and Richter,H.P. (1981) *Dev. Biol.*, **86**, 285-293.
Pitot,H.C. and Sirica,A.E. (1980) *Methods Cell Biol.*, **21B**, 441-456.
Renkin,E.M. (1954) *J. Gen. Physiol.*, **38**, 225-243.
Schatten,G. and Thoman,M. (1978) *J. Cell Biol.*, **77**, 517-535.
Seglen,P.O. (1976) *Methods Cell Biol.*, **13**, 29-83.
Sirica,A.E., Richards,W., Tsukuda,Y., Sattler,C.A. and Pitot,H.C. (1979) *Proc. Natl. Acad. Sci. USA*, **76**, 283-287.
Tanner,J.E. (1983) *Arch. Biochem. Biophys.*, **224**, 416-428.
Unwin,P.N.T. and Milligan,R.A. (1982) *J. Cell Biol.*, **93**, 63-75.
Wojcieszyn,J.W., Schlegel,R.A., Wu,E.-S. and Jacobson,K.A. (1981) *Proc. Natl. Acad. Sci. USA*, **78**, 4407-4410.

Received on 30 April 1984